ELSEVIER

Journal of Structural Geology 26 (2004) 1377–1390

JOURNAL OF STRUCTURAL GEOLOGY

www.elsevier.com/locate/jsg

Mechanical properties of multiphase materials and rocks: a phenomenological approach using generalized means

Shaocheng Ji[a,b,*], Qin Wang[a], Bin Xia[b], Denis Marcotte[a]

[a]*Département des Génies Civil, Géologique et des Mines, École Polytechnique de Montréal, Montréal, Canada, H3C 3A7*
[b]*Guangzhou Institute of Geochemistry, Chinese Academy of Sciences, Wushan, Guangzhou, P.R. China*

Received 11 August 2003; received in revised form 26 November 2003; accepted 9 December 2003

Available online 29 January 2004

Abstract

Difficulties associated with specifying details of microstructure and distributions of internal stress and strain within multiphase rocks prompt the development of semi-empirical models to connect the effective properties of composites to the properties of their components. We apply here generalized means to describe the elastic moduli (E, K and G) and flow strength of an isotropic multiphase composite material in terms of its component properties, volume fractions and microstructures. The microstructures are expressed by a scaling parameter J, which is mainly controlled by the shape and distribution (continuity and connectivity) of the phases. The case $J = 1$ yields the arithmetic mean or Voigt average and the case $J = -1$ yields the harmonic mean or Reuss average. The geometrical mean occurs as J approaches zero. The means with $J = -0.5$ or $J = 0.5$ provides good agreement with the experimental data of Young's modulus for the two-phase composites in which strong or weak inclusions are shaped like spheres isolated in a continuous host medium. For most composite materials in which the inclusions are of somewhat arbitrary geometry, the means with $J = -0.25$ and $J = 0.25$ do well at predicting the measured values of Young's modulus for those with weak-phase continuous (the volume fraction of strong phase $f_s \leq 0.5$) and strong-phase continuous ($f_s \geq 0.7$) structures, respectively. In the intermediate range ($0.5 \leq f_s \leq 0.7$), J is expected to vary progressively from -0.5 to 0.5 or from -0.25 to 0.25 due to the transition in microstructure. Thus the generalized means offer a promising, phenomenological approach for the prediction of elastic and rheological properties of multiphase materials and rocks, especially for those consisting of more than two unlike phases. As an example, the approach is applied to interpret the sharpness of the 410-km seismic discontinuity as a corollary of the transition from an olivine- to a wadsleyite-dominant structure.

Keywords: Generalized means; Elastic properties; Rheology; Multiphase rocks; Composite materials; Seismic discontinuities

1. Introduction

It is virtually impossible to obtain exact analytical solutions for mechanical properties (Young's modulus E, shear modulus G, bulk modulus K, and flow strength σ) of a multiphase mixture with a heterogeneous microstructure due to the fact that the local distributions of stress and strain of each constituent are influenced by the details of microstructure. Although advanced numerical techniques such as finite element modelling (e.g. Tullis et al., 1991; Treagus, 2002) have some inherent advantages for solving the above problem, they are too tedious to employ for each new composite. The numerical modelling results generally cannot be readily used in an efficient, straightforward manner in calculating the bulk mechanical properties of multiphase materials. Therefore, it is necessary to develop semi-empirical models to connect the overall properties of composites to the properties of their components. In this paper we use the generalized means as a phenomenological approach to calculate the elastic moduli (E, K and G) and flow strength of an isotropic composite material in terms of its component properties and volume fractions.

* Corresponding author. Correspondence address: Département des Génies Civil, Géologique et des Mines, École Polytechnique de Montréal, Montréal, Canada, H3C 3A7. Fax: +1-514-3403970.
E-mail address: sji@polymtl.ca (S. Ji).

0191-8141/$ - see front matter © 2004 Elsevier Ltd. All rights reserved.
doi:10.1016/j.jsg.2003.12.004

2. Mechanical properties of multiphase aggregates

The generalized (weighted) means can be expressed as:

$$M_c(J) = \left[\sum_{i=1}^{N}\left(f_i M_i^J\right)\right]^{1/J} \quad (1)$$

where M is a specific mechanical property (E, K, G, or σ), f is the volume fraction of component, the subscripts i and c represent, respectively, the ith phase and the composite consisting of N phases, and J is a scaling parameter.

$$\sum_{i=1}^{N} f_i = 1 \quad (2)$$

Here we propose that Eq. (1) is generically useful in the calculations of mechanical properties of multiphase materials. For example, the case $J = 1$ yields the arithmetic mean or Voigt average, which represents equal strain rate between phases. The case $J = -1$ yields the harmonic mean or Reuss average, which represents equal stress between phases. For statistically isotropic composites in which there is no mechanical interaction between phases (see Ji et al. (2000) for discussion), the Voigt and Reuss averages are generally regarded as the upper and lower bounds for effective properties and bracket the permissible range in which the effective properties must lie. The Voigt bound is linear with the volume fraction. The case $J = -1$ yields a formula like Wyllie's 'time-average equation' (Wyllie et al., 1956) for fluid-filled sedimentary rocks:

$$\frac{1}{V_c} = \frac{\phi}{V_1} + \frac{1-\phi}{V_2} \quad (3)$$

where V is a given seismic velocity, ϕ is the porosity, the subscripts 1, 2 and c represent, respectively, the fluid-filled pores, the solid medium and the composite. The Hill or the Voigt–Reuss–Hill average is an arithmetic mean of the Voigt and Reuss bounds (Hill, 1963).

Eq. (1) can be written as:

$$M_c^J = \sum_{i=1}^{N}\left(f_i M_i^J\right) \quad (4)$$

Taking the derivative of Eq. (4), and then let $J \to 0$, we have:

$$\ln M_c = \sum_{i=1}^{N} f_i \ln M_i = \sum_{i=1}^{N} \ln M_i^{f_i} = \ln\left(\prod_{i=1}^{N} M_i^{f_i}\right) \quad (5)$$

Eq. (5) clearly shows that as J approaches zero, the limit of $M_c(J)$ is the geometrical mean:

$$\lim_{J\to 0} M_c(J) = \prod_{i=1}^{N} M_i^{f_i} \quad (6)$$

The geometrical mean has been found to yield a result very close to the much more complicated iterative self-consistent micromechanical models (Matthies and Humbert, 1993; Mainprice and Humbert, 1994).

In the extreme cases, $M_c(J \to -\infty)$ and $M_c(J \to +\infty)$ define the minimum and the maximum, respectively. $M_c(J)$ has the following characteristics. (a) $M_c(J)$ is a continuous, monotone increasing function for all J in the ranges $(-\infty < J < \infty)$. This monotonicity stands with respect to either the volume fractions or the physical properties (Korvin, 1982). (b) For $J < 1$, $J = 1$ and $J > 1$, $M_c(J)$ as a function of the individual grades of membership M_i is strongly concave, linear, and strongly convex, respectively. (c) For a simple two-phase composite system that consists of the strong (s) and weak (w) phases, the generalized means fulfil the following obvious requirements: for $f_s = 0$ (pure weak phase aggregate), the effective properties are equivalent to the properties of the weak phase for all values of J. Similarly, for $f_s = 1$ (pure strong phase aggregate), the effective properties are equivalent to the properties of the strong phase for all values of J. In the event that $M_s = M_w$ (two phases have an equivalent property), then $M_c = M_s = M_w$ for all values of J and all values of f_s.

In Eq. (1), J can be viewed as a compensation coefficient whose value depends on characteristics of the composite microstructure such as the nature of interphase boundaries, phase continuity and connectivity. If the bonding between the phases is perfect, then the J value could be mainly controlled by the phase continuity and connectivity. Composites consisting of a strong and a weak constituent can be classified into three categories according to their phase continuity and connectivity (e.g. Gurland, 1979; Ji and Xia, 2002):

1. Composites with a strong-phase supported structure (SPSS), in which the strong phase is continuous while the weak phase is discontinuous in the direction of the applied load.
2. Composites with a weak-phase supported structure (WPSS), in which the strong phase is discontinuous while the weak phase is continuous in the loading direction.
3. Composites with a transitional structure (TS), in which both the strong and the weak phases are continuous or discontinuous in the loading direction.

The structures of granular materials generally depend on the volume fraction of constituent minerals. In hot-pressed forsterite–enstatite aggregates (Ji et al., 2001), for example, the SPSS, WPSS and TS occur, respectively, in composites with $f_s > 0.7$, < 0.5, and $0.5–0.7$. In addition to the volume fractions, the phase continuity and connectivity are of course affected by many other structural variables such as the morphology, grain size and the orientation of the constituents, which will be considered in a future study. The

phase continuity also changes with increasing progressive strain. A transition from SPSS to WPSS may result in a drastic decrease in effective elastic moduli or flow strength of the composites. This critical phenomenon has been used to explain the rheology of partially melted materials (e.g. Arzi, 1978; Rutter and Neumann, 1995) and solid-state rocks (e.g. Ji and Xia, 2002).

The overall mechanical properties can thus be estimated according to Eq. (1) if J is known. Then the problem at hand is to determine whether the J value is approximately constant for each of the structural categories. If J is a constant for a given type of structure, what is its value? The J value has to be determined by fitting the equation to experimental data.

3. Comparison with experiments

In order to test the theoretical model, high quality experimental data are needed for a series of macroscopically homogeneous and isotropic two-phase composites containing various known volume fractions of each constituent over a range as wide as possible. The polycrystalline aggregate of each end member phase should be isotropic so that only two elastic constants are necessary to characterize the bulk properties. These two elastic constants should be obtained by simultaneous measurements on the same specimen type in order to minimize effects due to experimental techniques and specimen variation. Any chemical interaction between phases or eutectic partial melting may introduce additional phases, consequently making the system complicated. The volume fraction of each phase should be accurately determined. For example, the presence of small amounts of residual void space (on the order of 1% by volume) is sufficient to make estimates of composite elastic constants (obtained while ignoring this porosity) fall below the lower Hashin–Shtrikman (HS) bound in many cases (Berryman, 1994, 1995). Furthermore, a shape preferred orientation may cause the composite to be anisotropic, but this effect can be avoided by using spherical particles in an isotropic matrix or random orientations of the grains. In addition, the contrast in elastic moduli between the phases should be large. Previous experimental checks of mixture rules (Watt and O'Connell, 1980; Ji and Wang, 1999) probably did not meet this criterion.

Elasticity and seismic velocities have been extensively measured for natural polyphase rocks (see Ji et al. (2002) for a comprehensive summary). However, such natural rocks are not optimal for the comparison between theory and experiment in order to determine the J value as a function of microstructure (e.g. phase continuity) primarily for the following reasons. (a) Natural rocks have complex mineralogical and chemical compositions and are rarely composed of only two minerals. (b) Natural rocks are generally anisotropic due to the presence of crystallographic preferred orientation and/or compositional layering. (c) Elasticity of each given natural composite system can hardly be determined over a full range of modal composition (Ji et al., 2003). (d) The volume fractions of constituent minerals reported for the rocks whose seismic velocities have been measured generally are not precise enough to yield an exact J value. It is thus especially important to determine the J value through carefully designed experiments using synthetic two-phase aggregates of well-controlled modal compositions and microstructures. Unfortunately, such elastic data are still very scarce for synthetic multiphase rocks. Thus, the elastic properties predicted by the expressions proposed in this paper were compared with the experimentally measured values of various synthetic composites, reported in the materials science and geophysics literature, in order to constrain the J value and its variation with composition.

3.1. SPSS composites

Porous materials are a special class of SPSS composites in which pores are dispersed within a continuous nonporous body. Pores act like a constituent with null elastic constants. Porous powder metals, ceramics, sedimentary rocks and cracked rocks belong to this category. Powder metals and ceramics are usually manufactured by sintering or hot pressing. Polyphase materials in which the weak phases are at least two orders of magnitude weaker than the strong phases (e.g. partially melted rocks) can also be regarded as an analogy of porous materials (Arzi, 1978; Tharp, 1983; Ji and Xia, 2002). In Eq. (1), setting the elastic properties of a phase equal to zero allows an estimation of the effect of porosity on elastic properties of porous materials. As shown in Fig. 1, the relative Young's modulus calculated from Eq. (1) and using $J = 0.25$ are in good agreement with experimental data for porous Al_2O_3 (Spriggs, 1961; Knudson, 1962) and porous MgO (Spriggs et al., 1962) polycrystalline aggregates with porosities less than about 40% (i.e. $f_s > 60\%$). The relative Young's modulus is defined as $(E_c - E_w)/(E_s - E_w)$, where E_s, E_w and E_c are the Young's moduli of the strong phase, weak phase and the composite, respectively. For porosities less than 20%, the discrepancy between the experimental and theoretical results predicted with $J = 0.25$ is no more than a few percent. In contrast, the Hill average cannot yield a good fit to the experimental data. Thus, $J = 0.25$ is apparently an appropriate assumption for the porous Al_2O_3 and MgO investigated.

Walsh et al. (1965) carried out a series of experiments on the compressibility ($1/K$) of porous glass (glass foams) over a range of porosities from 0 to 0.7. The glass has the composition (in weight) 54.4% SiO_2, 14.4% B_2O_3, 14.1% CaO, 10% Al_2O_3, 6.5% Na_2O and 0.7% K_2O, $K = 46$ GPa and $G = 30.5$ GPa. Porosity measurements were stated to be accurate to ± 0.01. The experimental data are plotted in Fig. 2 for comparison with the theoretical relation proposed in the present paper and with the Hashin–Shtrikman (HS)

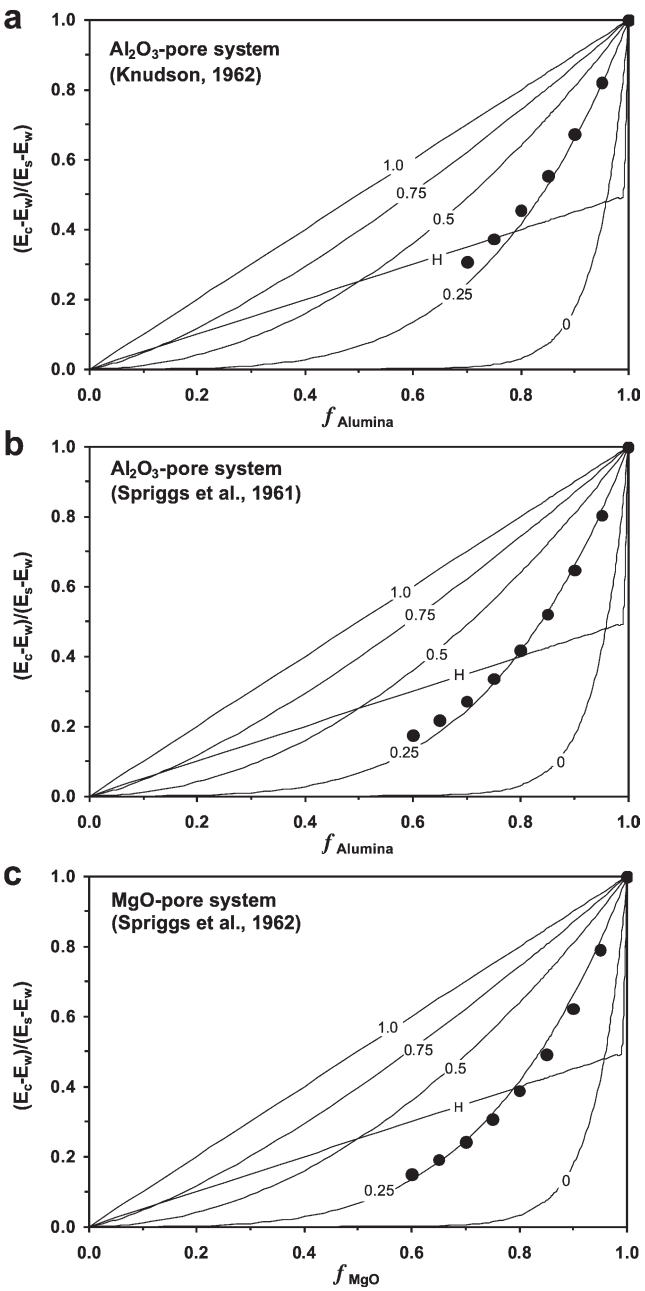

Fig. 1. Experimental and theoretical results for relative Young's modulus of porous Al_2O_3 ((a) and (b)) and MgO (c) as a function of the volume fraction of solid component. Curves labelled according to J value. H represents the Hill average.

bounds. The upper and lower HS bounds were derived by Hashin and Shtrikman (1963) using a linear theory of elasticity with the elastic polarization tensor method. In their derivation, potential energy and complementary energy were assumed to be minimum. The experimental data of Walsh et al. (1965) essentially track the theoretical curve of $J = 0.5$ for samples of low or immediate porosity ($f_s \geq 0.5$). In these samples, the pores are nearly spherical and non-interconnecting (Walsh et al., 1965). It is clear that the geometry of pore space is another important factor other than the phase continuity to affect the J value and further

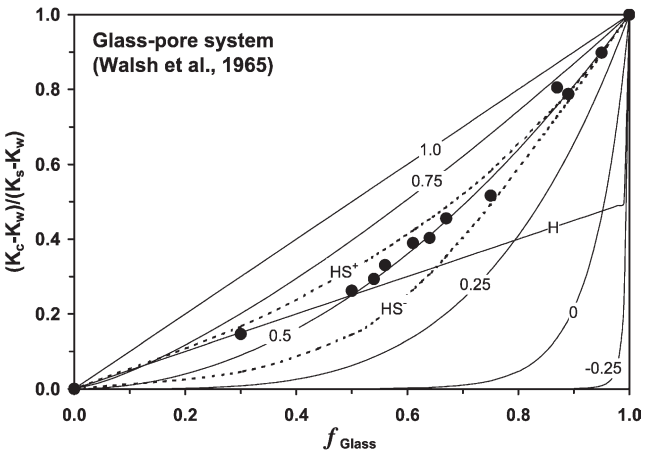

Fig. 2. Comparison between experimental and theoretical results for relative bulk modulus $(K_c - K_w)/(K_s - K_w)$ for glass foams. Theoretical curves labelled according to J value. H, HS^+ and HS^- represent the Hill average, and the Hashin–Shtrikman upper and lower bounds, respectively.

elastic properties of the composite. Isolated spherical pores cause the J value to be higher than sharp-cornered holes or flat elliptical cavities. Likely, $J \approx 0.5$ for the case of identically spherical pores while $J \approx 0.25$ for that of non-spherical or non-symmetric cavities. Fig. 2 also displays that the model with $J = 0.5$ yields a better prediction than the upper HS bound in the case of the porous glass investigated by Walsh et al. (1965).

Berge et al. (1995) made measurements on P- and S-wave velocities of synthetic sandstone using sintered glass beads with porosities ranging from 1 to 43%. The glass has composition (by weight) 71–74% SiO_2, 12–15% NaO_2, 8–10% CaO, 1.5–3.8% MgO, 0.2–1.5% Al_2O_3 and 0–0.2% K_2O, and elastic properties $K = 46.1$ GPa, $G = 29.8$ GPa, $\rho = 2.48$ g/cm^3, $V_p = 5.86$ km/s and $V_s = 3.43$ km/s. The overall Young's, bulk and shear moduli of composites were computed from measured densities and acoustic velocities. Comparison between theory and experiment (Fig. 3) shows a clear drop of the relative E, G and K towards a critical porosity of about 0.26. For porosities below about 0.26 ($f_s > 0.74$), the samples have similar microstructures with isolated spherical pores embedded in a continuous solid glass (Berge et al., 1995) and the experimental data can be well described by the generalized means with $J = 0.5$ or by the upper HS bound. The critical porosity presumably coincides with the minimum porosity for closely packed identical spheres. In Fig. 4, we plot measured P- and S-wave velocities of the sandstone analogues together with the theoretical predictions. Both P- and S-wave velocities of synthetic sandstone containing isolate pores and having porosities lower than 0.26 are in agreement with the theoretical curves for $J = 1.5$. In sandstones with higher porosities (0.26–0.43), the geometry of pores becomes complex and interaction between pores occurs. Consequently, the J value decreases progressively with increasing porosity. It is important to note that both P- and S-wave velocities of the composites with SPSS are virtually higher

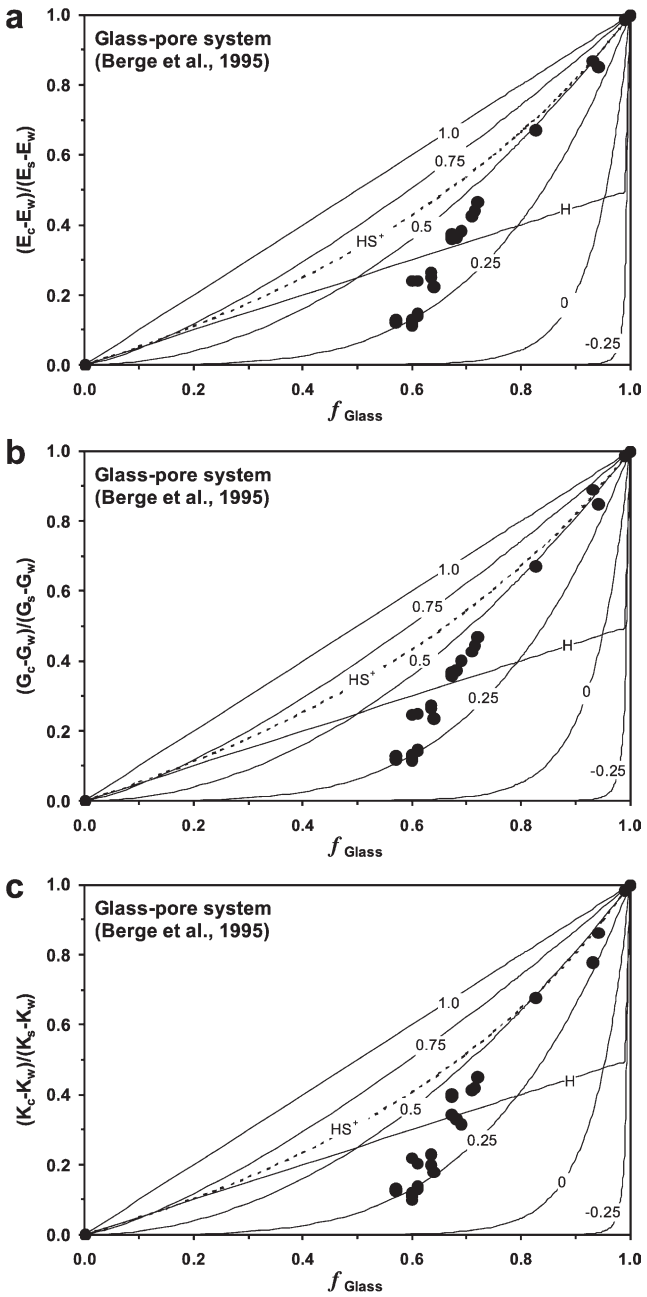

Fig. 3. Comparison between experimental and theoretical results for relative Young's modulus (a), shear modulus (b) and bulk modulus (c) for sandstone analogues made from fused glass beads. Theoretical curves labelled according to J value. H and HS^+ represent the Hill average and the Hashin–Shtrikman upper bound, respectively.

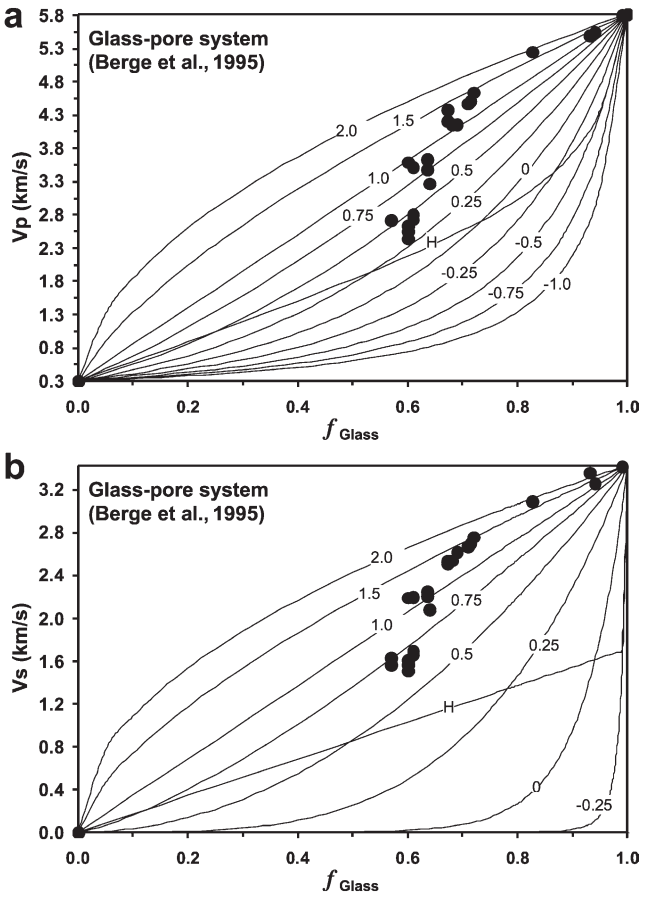

Fig. 4. P-wave (a) and S-wave (b) velocities for sandstone analogues made from fused glass beads plotted against volume fraction of solid glass. Theoretical curves labelled according to J value. H represents the Hill average.

than the Voigt bounds ($J = 1$). Hence, a systematic investigation is urged to determine whether the above observation is a common situation for all types of materials.

In Figs. 5 and 6, the theoretical predictions are plotted in junction with experimental data for WC–Co cermets (Doi et al., 1970; Perrott, 1978). $E = 700$ GPa and $G = 297.9$ GPa for WC, and $E = 207$ GPa and $G = 79.4$ GPa for Co. In these alloys, the volume fraction of WC (strong phase) is higher than 0.55 and Co (weak phase) shows a homogeneous dispersion in the matrix of WC. It can be clearly seen that the simple expression with $J = 0.25$ gives a good prediction of both the E and K variations over the composition range of $f_{WC} > 0.55$, where the strong phase forms a continuous load-carrying framework. For the shear modulus G, however, $J = 0$ (i.e. geometrical mean) seems to give the best prediction for the experimental data. The reason for the discrepancy among the E, K and G variations with the volume fractions is unclear yet.

3.2. WPSS composites

Extensive measurements of elastic properties have been carried out on WPSS composites that include Al–SiC, glass–Al_2O_3, epoxy–glass, epoxy–silica, epoxy–Al, polymer–glass, Al–spinel and Al alloy–boron mixtures. These experimental results may shed light on the understanding of the mechanical properties and rheological behaviour of natural rocks of WPSS such as quartzofeldspathic mylonites, peridotites, eclogites and partially crystallized rocks.

Utilizing the values of Young's moduli of Al ($E_w = 74$ GPa) and SiC ($E_s = 450$ GPa) and Eq. (1), we made some quantitative comparisons of the Young's moduli

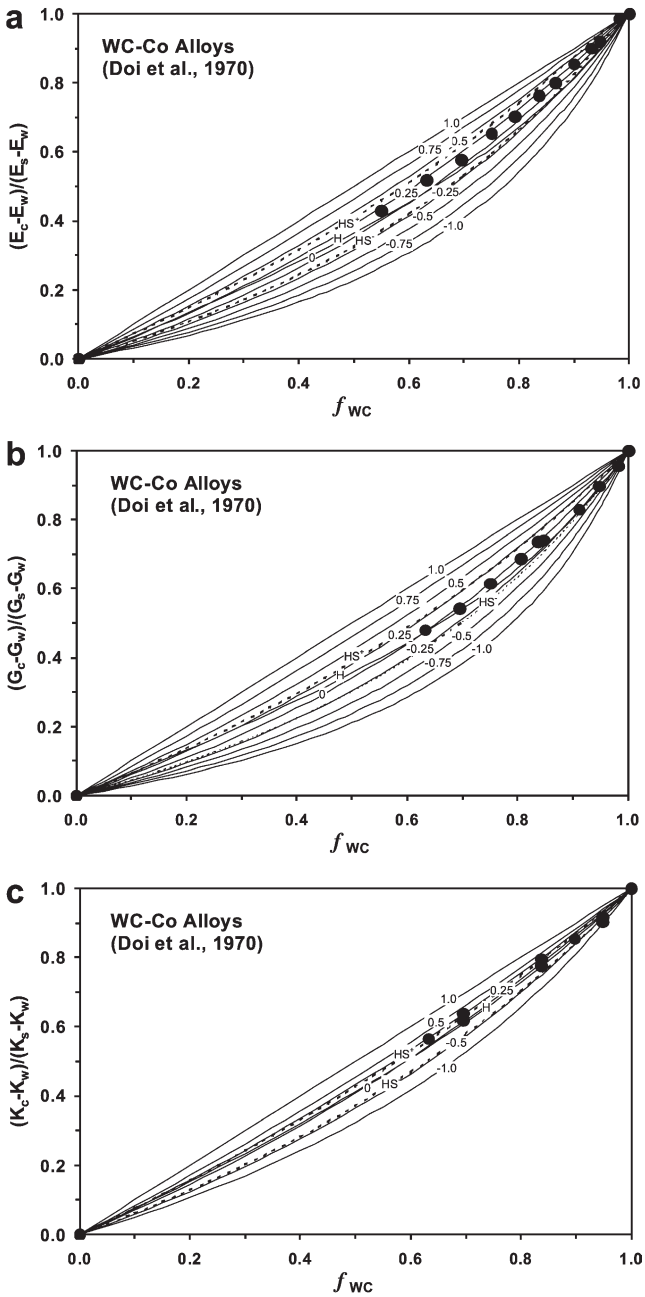

Fig. 5. Relative Young's modulus (a), shear modulus (b) and bulk modulus (c) for WC–Co alloys plotted against volume fraction of WC. Theoretical curves labelled according to J value. H, HS^+ and HS^- represent the Hill average, and the Hashin–Shtrikman upper and lower bounds, respectively.

between theory and experiment (McDanels, 1985; Lloyd, 1991; Yang et al., 1991) for Al–SiC composites (Fig. 7a and b). The experimental points of Young's moduli run very closely to the curves for $J = -0.25$. The composition dependence of Young's moduli of Al matrix composites with boron (Chen and Lin, 1969; Fig. 7c) or spinel (Gustafson et al., 1997; Fig. 8a) reinforcements also suggests that $J = -0.25$ gives the best prediction for the experimental results. However, the experimental points for

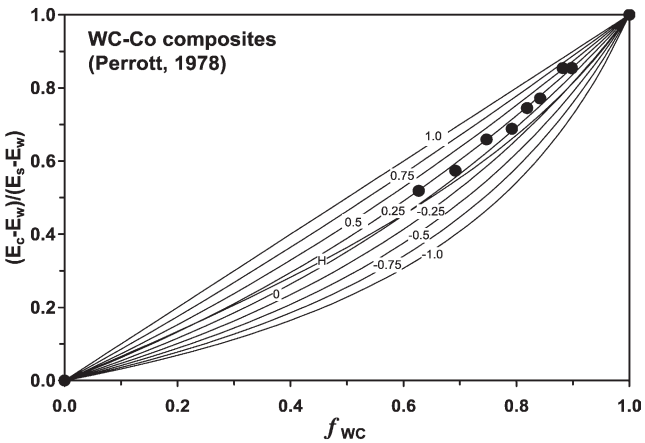

Fig. 6. Relative Young's modulus for WC–Co alloys plotted against volume fraction of WC. Theoretical curves labelled according to J value. H represents the Hill average.

G and K of Al–spinel composites (Fig. 8b and c) fall closely to curves with $J = 0$ and $J = -1.5$, respectively.

Composites composed of solid glass or silica microspheres embedded in an epoxy resin or polymer matrix have been investigated by Braem et al. (1987), Ishai and Cohen (1967), Kenyon and Duffey (1967), Richard (1975) and Smith (1976). These experimental data are plotted among the analytical predictions for different J values in Figs. 9 and 10. In all cases, the prediction with $J = -0.25$ provides the best fit to the experimental data of Young's moduli. It is interesting to note that the calculated Young's moduli from either the upper or lower HS bound in all cases have larger deviations from experimental data than those calculated from Eq. (1) with $J = -0.25$. Fig. 10c shows a good correlation of the experimental data of bulk modulus with the theoretical prediction with $J = -1.5$. This is similar to the case of Al–spinel composites (Fig. 8c). Why do the data of K fall outside the HS bounds while both E and G inside the bounds for certain types of materials such as Al–spinel (Gustafson et al., 1997) and epoxy–glass (Richard, 1975) composites? Without a detailed examination of their samples, we can only speculate that the paradox is due to the presence of small amounts of residual void space in the samples that are treated for purposes of modelling as if they have no porosity (Berryman, 1994, 1995).

Zhang et al. (1996) investigated the effective elastic properties of a two-phase composite consisting of aluminum particles embedded randomly in a continuous resin matrix. Bulk and shear moduli for aluminum are 77.44 and 24.77 GPa, respectively. Bulk and shear moduli for resin are 5.31 and 1.82 GPa, respectively. The shapes of the Al inclusions are elongate with aspect ratios (width/length) ranging from 0.1 to 1.0, averaging about 0.25. The bulk, shear and Young's moduli of the composites, obtained from velocities of ultrasonic waves, are plotted in Fig. 11. The observed relative Young's and shear moduli can be best fitted by the theoretical curve of $J = -0.25$ (Fig. 11a and b). In contrast, the relative bulk modulus is best fitted by the

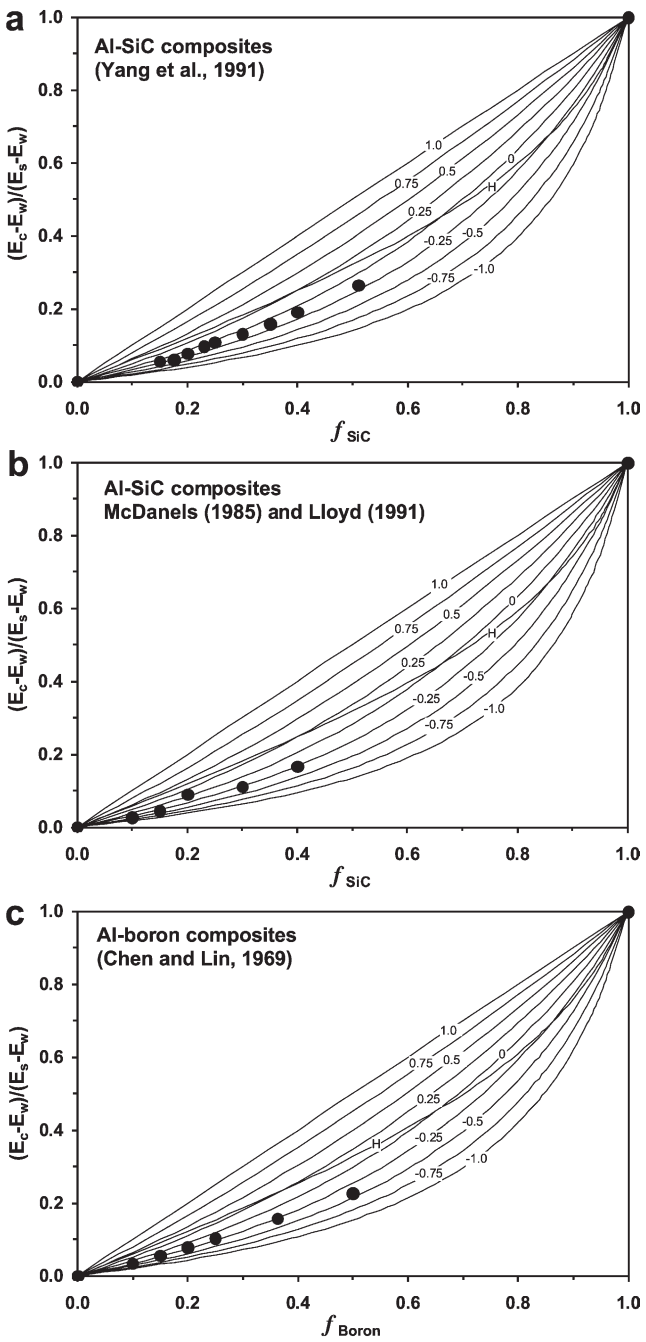

Fig. 7. Theoretical curves on relative Young's modulus $(E_c - E_m)/(E_s - E_m)$ for aluminium–matrix composites plotted against volume fraction of reinforcement. Al–SiC composites ((a) and (b)) and Al–boron composites (c). J value is given in number. H represents the Hill average.

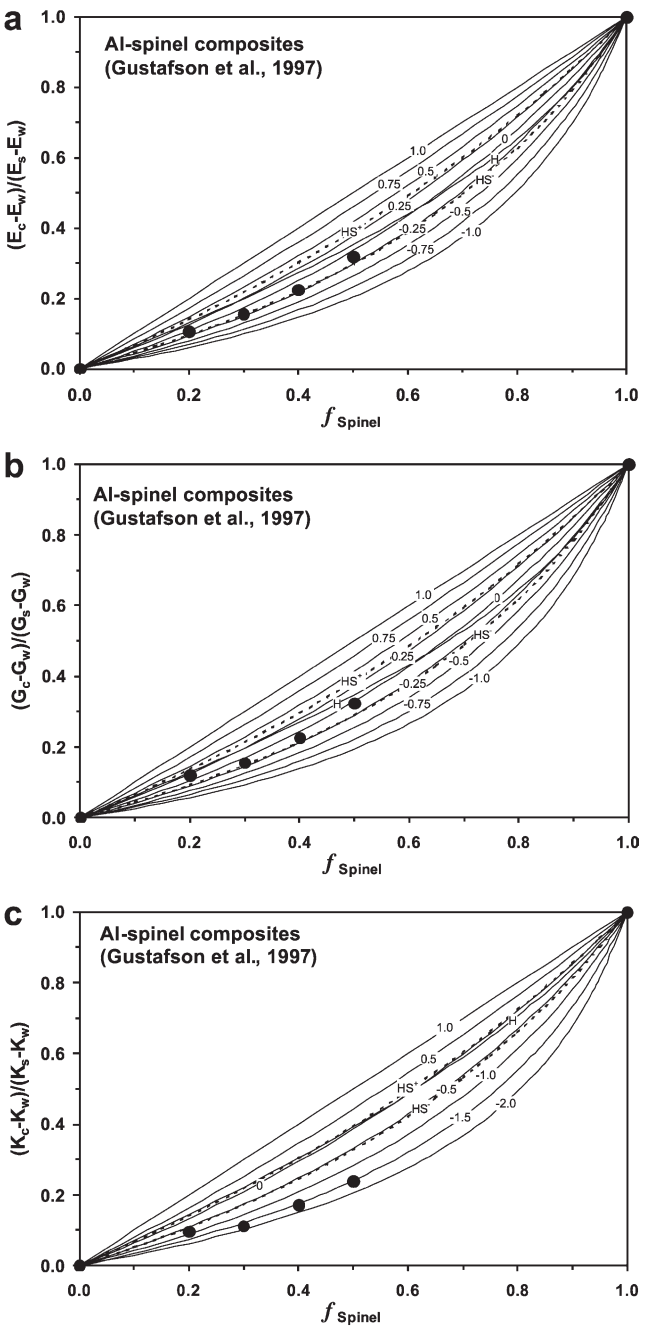

Fig. 8. Relative Young's modulus (a), shear modulus (b) and bulk modulus (c) for Al–spinel composite plotted against volume fraction of spinel. Theoretical curves labelled according to J value. H, HS^+ and HS^- represent the Hill average, and the Hashin–Shtrikman upper and lower bounds, respectively.

theoretical curves of $J = -0.5$ (Fig. 11c). In addition, measured P- and S-wave velocities of the composites (Fig. 12) correspond to theoretical curves of $J = -2.0$ and -1.0, respectively. Hence, even for the composites with the same composition and same microstructure, J values are different for different elastic moduli or mechanical properties. This aspect should receive a further detailed study.

Glass–Al_2O_3 composites investigated by Hasselman and Fulrath (1965a) are characterized by a sodium borosilicate glass (16% Na_2O, 14% B_2O_3 and 70% SiO_2) containing dispersions of alumina particles. The composite aggregates were prepared using a vacuum hot-pressing technique at 725 °C. The alumina particles, which are crushed sapphire, are quite jagged and nonspherical in shape and have a mean particle size of about 50 μm. The Young's moduli for the glass and the alumina are 80.5 and 411 GPa, respectively (Hasselman and Fulrath, 1965a). The Poisson's ratios of the

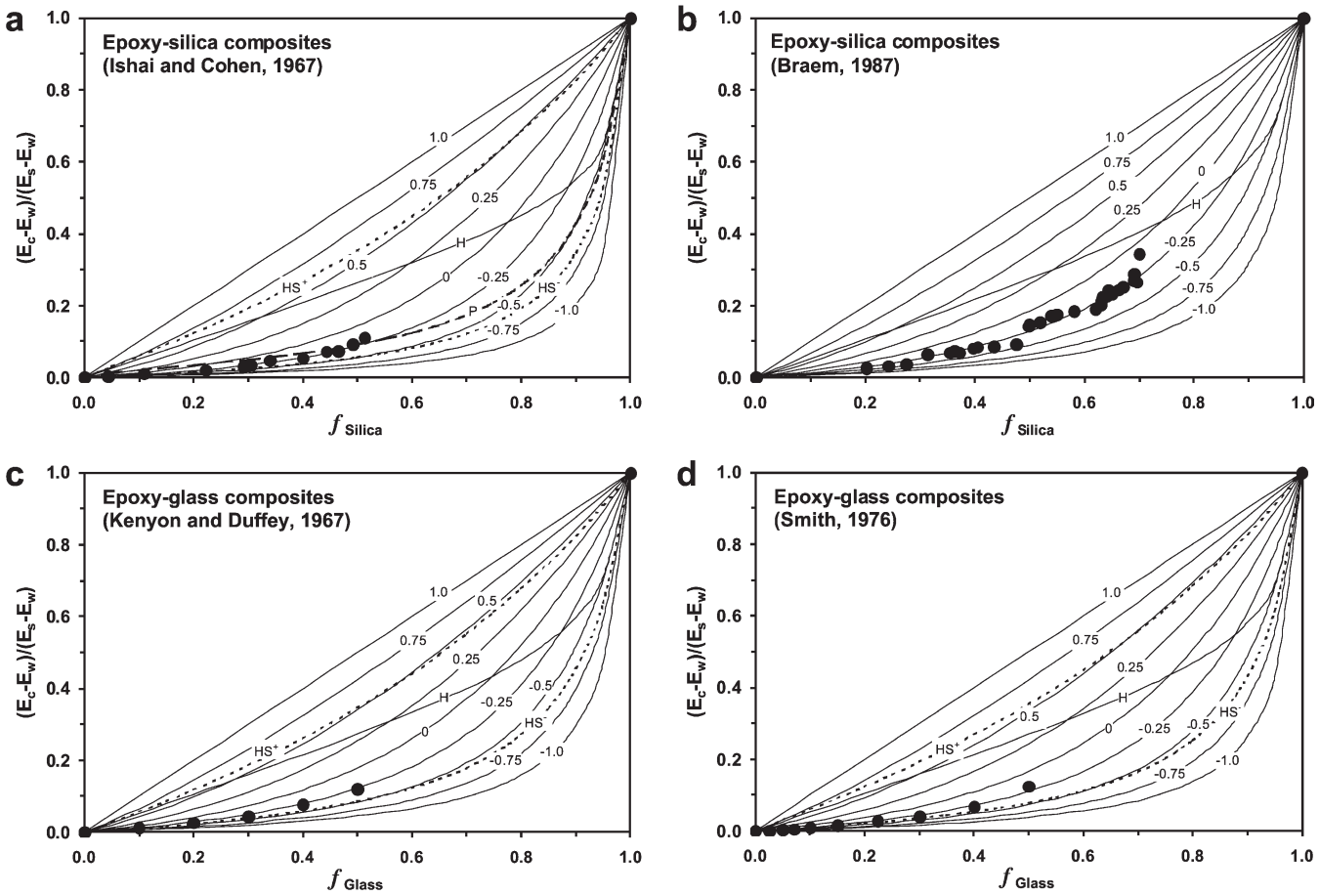

Fig. 9. Comparison of the predictions of the present approach, the Hashin–Shtrikman upper (HS^+) and lower (HS^-) bounds, Paul's (1960) calculations (P) with experimental data on relative elastic Young's moduli of epoxy resin-based composites. Epoxy–silica composites ((a) and (b)) and epoxy–glass composites ((c) and (d)). J value is given in number. H represents the Hill average.

glass and the alumina are 0.194 and 0.257, respectively. As shown in Fig. 13a, the theoretical curve with $J = -0.25$ tracks the lower HS bound at $f_s \leq 0.4$, where both predictions agree very well with the experimental results. At higher f_s, however, the generalized means give definitely better agreement with the data than the lower HS bound.

Hasselman and Fulrath (1965b) also measured the Young's moduli of glass–tungsten composites with $f_s \leq 0.5$. The Young's moduli and Poisson's ratios for the glass and the tungsten are 80.5 and 355 GPa and 0.197 and 0.198, respectively. There is a good consistence between their experimental results and our theoretical curve with $J = -0.25$ (Fig. 13b). Similarly, the generalized means provide a better prediction than the lower HS bound. Thus, a good agreement of the calculated and experimental data for a large number of two-phase composite systems evaluated above supports that $J = -0.25$ for predicting effective Young's modulus of the composites with WPSS.

Einstein (1906, 1911) theoretically analysed the rheology of a specific WPSS composite, which is a dilute suspension of identical rigid spheres in a Newtonian viscous liquid, and obtained:

$$\eta_c = \eta_w\left(1 + \frac{5}{2}f_s\right) \tag{7}$$

where η_c and η_w are the bulk viscosity of the suspension and the viscosity of the liquid, and f_s is the volume fraction of rigid spheres. In the dilute system, each single sphere is isolated in the continuous liquid matrix, and no slip occurs between the spheres and the liquid. This famous Einstein equation, which agrees with many experimental data (e.g. Mewis and Macosko, 1994), has been widely used in the rheological study of solid–liquid suspensions such as partially melted rocks (Arzi, 1978; Lejeune and Richet, 1995). As shown in Fig. 14, the generalized means with $J = -0.5$ yield a very close approximation to the Einstein equation with a relative error less than 1% as long as the two phase composite is a really dilute suspension (i.e. $f_s \leq 0.15$). The above comparison again suggests that $J = -0.5$ for the WPSS composites with their strong phases are identically spherical.

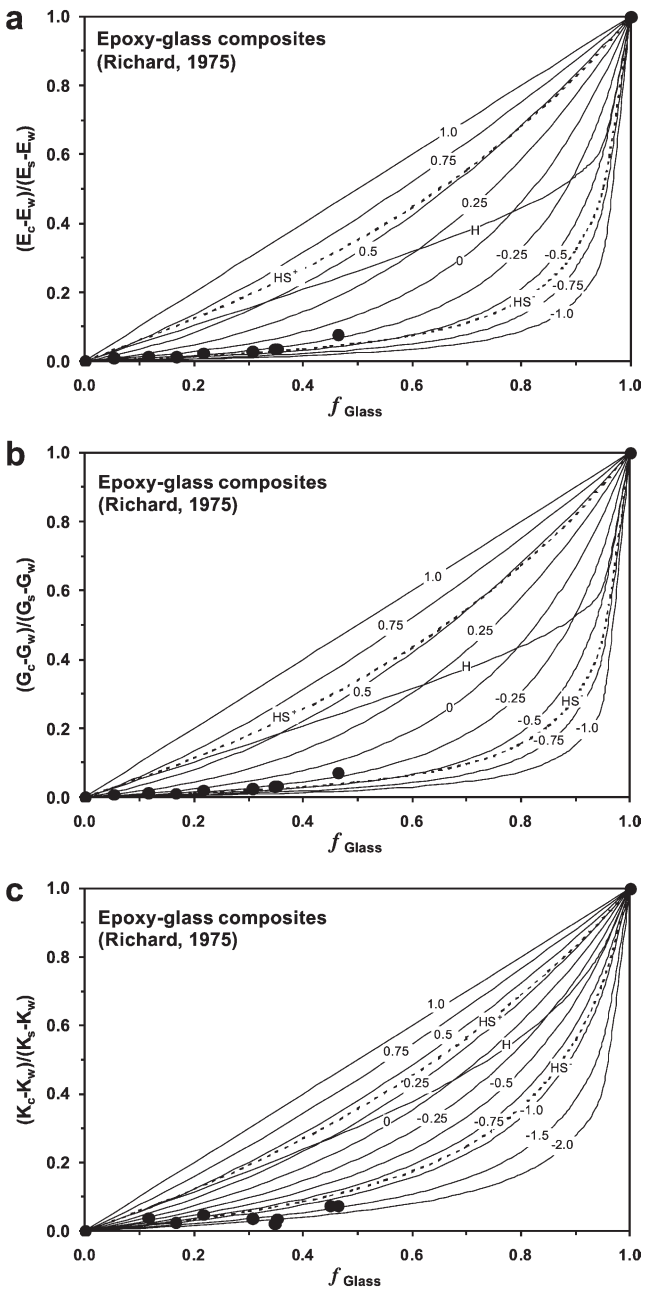

Fig. 10. Comparison of the predictions of the present approach, the Hashin–Shtrikman upper (HS^+) and lower (HS^-) bounds with experimental data on relative Young's modulus (a), shear modulus (b) and bulk modulus (c) of epoxy–glass composites. J value is given in number. H represents the Hill average.

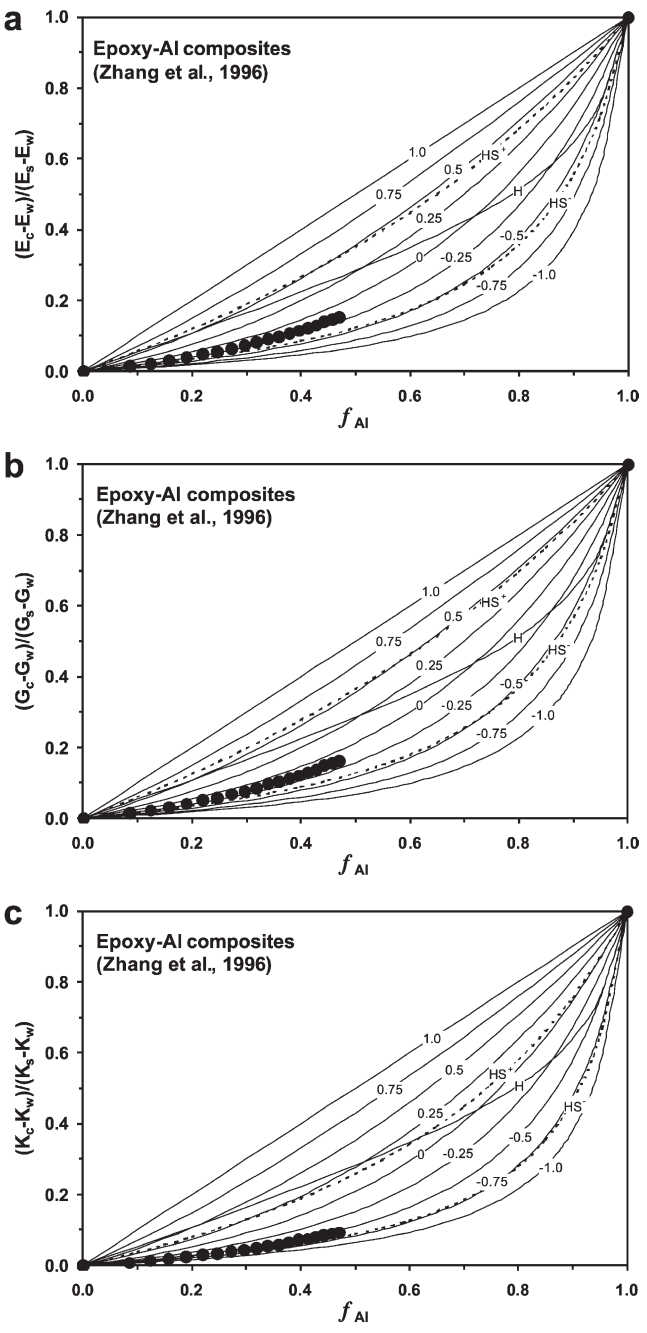

Fig. 11. Relative Young's modulus (a), shear modulus (b) and bulk modulus (c) for epoxy–Al composite plotted against volume fraction of Al. Theoretical curves labelled according to J value. H, HS^+ and HS^- represent the Hill average, and the Hashin–Shtrikman upper and lower bounds, respectively.

4. Application to the interpretation of 410-km seismic discontinuity

The seismic discontinuity at 410 km depth is considered to be caused by a phase transition of the main constituent of the upper mantle–olivine to wadsleyite (i.e. modified spinel or β phase of $(Mg, Fe)_2SiO_4$; Lebedev et al., 2002). Seismological studies using high-frequency reflected and converted waves indicate that this discontinuity has a width of less than 4–6 km (Leven, 1985; Paulssen, 1988; Benz and Vidale, 1993), which is much too thin to be explained by the depth interval (~14 km corresponding to 0.5 GPa at 1600 °C; Akaogi et al., 1989; Katsura and Ito, 1989; Fei et al., 1991) over which olivine transforms fully to wadsleyite. A number of hypotheses have been proposed to explain why the phase transition is much sharper than the prediction based on the width of the binary coexistence region. These hypotheses include:

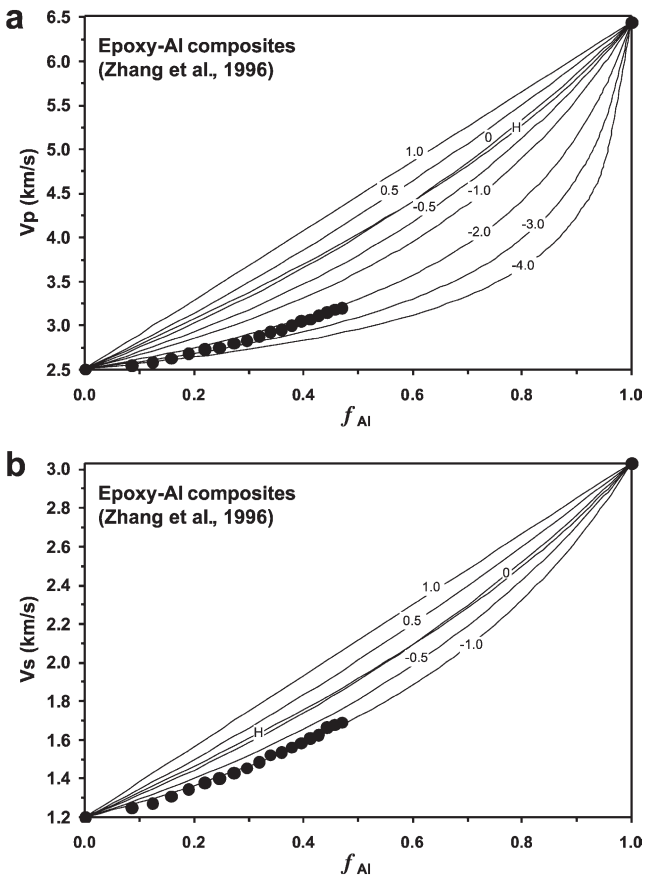

Fig. 12. P-wave (a) and S-wave (b) velocities for epoxy–Al composites plotted against volume fraction of Al. Theoretical curves labelled according to J value. H represents the Hill average.

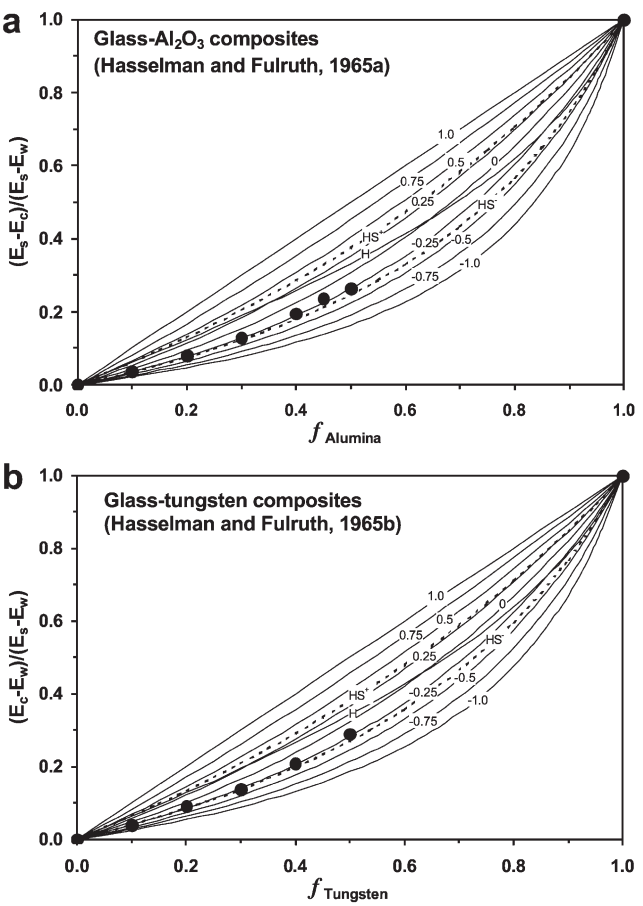

Fig. 13. Theoretical curves on relative Young's modulus $(E_c - E_w)/(E_s - E_w)$ for glass–matrix composites plotted against volume fraction of reinforcement. Glass–Al_2O_3 composites (a) and glass–tungsten composites (b). Theoretical curves labelled according to J value. H, HS^+ and HS^- represent the Hill average, and the Hashin–Shtrikman upper and lower bounds, respectively.

1. Seismic discontinuities originate from so-called univariant phase transitions that occur suddenly at a very narrow pressure interval (Jeanloz and Thompson, 1983). However, the chemical system of the upper mantle is multicomponent, and simple phase relations show that the transition from olivine to wadsleyite must occur in a divariant loop (Wood, 1995). Furthermore, for a univariant phase transition to produce the 410-km discontinuity, the Fe content of the upper mantle should be substantially different from that generally accepted on the basis of geochemical data from mantle xenoliths (Stixrude, 1997).
2. Seismic discontinuities are caused by a change not only of phase but also of composition (Lees et al., 1983; Bina and Kumazawa, 1993) over a narrow depth interval. As pointed out by Stixrude (1997), however, the formation of a well developed compositional stratification in the upper mantle would require large chemical diffusivities that, in turn, require substantial amounts of fluids.
3. Seismic discontinuities are caused by phase transitions that occur under non-equilibrium conditions in a dynamic system (Solomatov and Stevenson, 1994). This mechanism is most likely to occur in subducting slabs rather than in most of the mantle.
4. The volume fraction of the high-pressure phase (generally elastically stiffer) increases nonlinearly with temperature and pressure so that most of the phase transition is completed over a narrow depth interval (Stixrude, 1997).

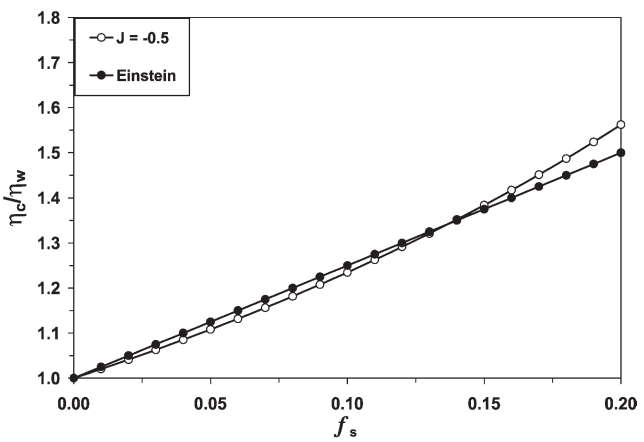

Fig. 14. Comparison between the predictions of the present approach and the Einstein equation for the relative viscosity of a suspension as a function of identically spherical, solid inclusions.

5. Non-transforming phases such as pyroxenes and garnet act as buffers to reduce the total width over which a transition occurs (Stixrude, 1997).
6. The paradox is due to the difference in H_2O content between actual upper mantle and experimental samples because the pressure interval of the olivine to wadsleyite transformation increases with increasing the H_2O content (Wood, 1995).

In all the above models, the width of the phase transition is taken as controlled by the width of the coexistence region (i.e. equilibrium phase loop of Stixrude, 1997). Here we propose that the sharpness is essentially governed by a critical high-pressure phase volume fraction range over which the transition is completed from weak-phase supported structure (WPSS) to strong-phase supported structure (SPSS). When olivine progressively transforms to wadsleyite with increasing depth in the transition zone, an increase in wadsleyite volume fraction is accompanied by a change in microstructure (i.e. phase continuity and connectivity). The composition dependence of the elastic moduli then cannot be expressed by an equation like Eq. (1) with a single J value valid over the whole range of $f_{\text{wadsleyite}}$ from zero to unity. Fig. 15a and b illustrates the variation of P- and S-wave impedances for olivine–wadsleyite mixtures due to the WPSS to SPSS transition. For the SPSS mixtures, the impedance varies with wadsleyite volume fraction according to curve ABCD. For the WPSS mixtures, however, the impedance varies with wadsleyite volume fraction according to curve DEFA. When the volume fraction of wadsleyite reaches a critical value, say about 40–45%, the olivine frame begins to be progressively dismembered by wadsleyite grains. After the volume fraction of wadsleyite is larger than a second critical value, say 70–75%, olivine grains are fully dispersed as residuals in a continuous matrix of wadsleyite. Therefore, there is an evolution in seismic impedance for the olivine–wadsleyite mixture from D, through E and B, finally to A (Fig. 15) during progressive olivine to wadsleyite transformation with increasing pressure or depth.

No model is available for describing the elastic properties or flow strength of two-phase composites in the transitional regime (Ji et al., 2001). Let M_1, f_1 and M_2, f_2 be the overall elastic moduli and the strong phase volume fractions at the lower and upper boundaries of the transition range (E and B points in Fig. 15), respectively. We assume that a mathematic expression, $M_c(f_s)$, for the transitional regime should be constrained by the following conditions: (1) $M_c(f_s)$ is a continuous, monotonically increasing function in the range from f_1 to f_2; (2) $M_c = M_1$ at $f_s = f_1$ and $M_c = M_2$ at $f_s = f_2$; (3) the curve $M_c(f_s)$ is symmetrical with respect to the mid-point where $f_s = (f_1 + f_2)/2$ and $M_c = (M_1 + M_2)/2$, therefore, $M_c(f_s)$ is an odd function of f_s and

$$M_c\left(f_s - \frac{f_1+f_2}{2}\right) = -M_c\left(\frac{f_1+f_2}{2} - f_s\right);$$

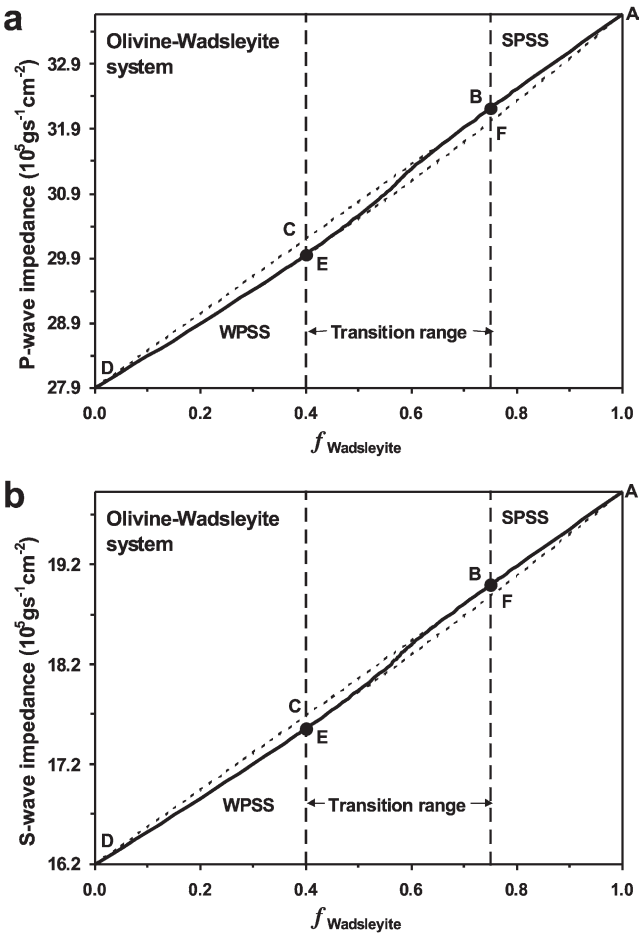

Fig. 15. Variation of P-wave (a) and S-wave (b) impedances for olivine–wadsleyite system with its composition for three typical structures: curve ABCD, discontinuous weak phase (olivine) grains in continuous strong framework of wadsleyite; curve DEFA, discontinuous strong phase (wadsleyite) embedded in a continuous weak matrix; curve EB, calculated from Eq. (8) with $J = 0.5$ and $k = 1.1$, both phases are either discontinuous or continuous and there is a transition from an olivine-dominant configuration to a wadsleyite-dominant configuration with increasing the volume fraction of wadsleyite (from E to B).

and (4) $M_c(f_s)$ is concave when $f_s \le (f_1 + f_2)/2$, and convex when $f_s \ge (f_1 + f_2)/2$. The simplest expression that satisfies with the above limiting conditions is the following smooth function:

$$M_c = \frac{M_1 + M_2}{2} + \delta\frac{M_2 - M_1}{2}\left(\frac{\left|f_s - \frac{f_1+f_2}{2}\right|}{\frac{f_2-f_1}{2}}\right)^{1/k} \tag{8}$$

where k is an odd number, $\delta = 1$ when $f_s \ge (f_1 + f_2)/2$, and $\delta = -1$ when $f_s \le (f_1 + f_2)/2$. Although Eq. (8) is certainly not a unique solution to the limiting conditions, we could not find any additional constraints to warrant the use of a more complicated expression.

The P- and S-wave impedance contrasts are about 3.6%, across the critical $f_{\text{wadsleyite}}$ range over which WPSS transforms to SPSS. This impedance contrast agrees with the value in the preliminary reference Earth model (Dziewonski and Anderson, 1981). The volume fraction range for the WPSS to SPSS transition is only one third the width of the olivine − wadsleyite coexistence region. This means that the effective width of the seismic discontinuity at 410 km mainly indicates the width of the transition from olivine-supported structure to wadsleyite-supported structure rather than that of a full experimentally determined binary phase loop. The latter is substantially larger than the actual width of the seismic discontinuity. For temperatures and pressures in a typical transition zone the effective width of the WPSS to SPSS transition lies between 4 and 6 km. This agrees with the maximum width of an equivalent linear discontinuity (4–6 km) found in reflections from the 410-km discontinuity (Leven, 1985; Benz and Vidale, 1993).

When effects of the structural transition on the effective elastic properties of multiphase mixtures are taken into account, the transition from olivine to wadsleyite is sufficient to explain the sharp seismic discontinuity at 410-km depth, and any other special processes or properties implied in models (1–6) are not required. It may be reasonable to conclude that any seismic discontinuity due to phase transformations has a width equivalent to that of the transition between WPSS and SPSS and being about a quarter to a third of the width of the binary phase loop. Therefore, the sharpness of the 410-km seismic discontinuity is a corollary of the transition from olivine-dominant structure to wadsleyite-dominant structure.

5. Discussion and conclusions

The elastic properties of multiphase composites can be calculated according to the simple expression proposed in this paper, which involves utilization of the generalized means. The approach is believed to be relevant if one phase is a homogeneous and isotropic continuum (the matrix) with embedded inclusions of the other phase, which is also homogeneous, isotropic and randomly distributed through the matrix. The approach postulates neither untested nor poorly constrained physical properties or processes (e.g. isostrain or isostress), nor any approximation of composite microstructure to an idealized, somehow oversimplified unit cell (e.g. Tullis et al., 1991; Treagus, 2002). The calculations require only the knowledge of the elastic modulus and the volume fraction of each individual phase and a pertinent value of the microstructural parameter J. The means with $J = 0.5$ or $J = -0.5$ provides good agreement with the experimental data of Young's modulus for the two-phase composites in which inclusions are shaped like spheres isolated in a continuous host medium (Table 1). For most composite materials in which the inclusions are shaped somewhat randomly, the means with $J = -0.25$ and $J = 0.25$ do well at predicting the measured values of Young's modulus for those with weak-phase continuous (the volume fraction of strong phase $f_s \leq 0.5$) and strong-phase continuous ($f_s \geq 0.7$) structures, respectively (Table 1). In the intermediate compositional range ($0.4–0.5 \leq f_s \leq 0.6–0.7$), J most likely varies progressively from -0.5 to 0.5 or from -0.25 to 0.25 due to the transition in microstructure. Thus we believe that the generalized means offer a great potential for providing useful predictive relationships between the composite properties and the component contents for various multiphase materials and rocks.

The coefficient J in the generalized mean formula is shown to be constant for a given elastic modulus of composites of a particular microstructure, regardless of the elastic contrast between constituent phases. Thus, the J value is referred to as a microstructural coefficient, which depends on the shape and distribution (continuity and connectivity) of the phases. For isotropic granular materials and rocks, the phase continuity and connectivity are a function of phase volume fractions, and therefore the J value should depend on the phase volume fractions. The J value changes when a weak-phase supported structure transforms to a strong-phase supported structure. Furthermore, for a multiphase material with a constant microstructure, different J values may be needed to describe different mechanical properties. Hence, a systematic study is urged to determine the J values for G, K, P- and S-wave velocities, viscosity and flow strength.

The theoretical values of Young's modulus for composites with weak phase support structure and strong phase support structure coincide nearly with the commonly used Hashin and Shtrikman's (1963) lower and upper bounds, respectively. The theoretical values calculated with $J = -0.25$ also agree well with Paul's (1960) model for arbitrary phase geometry. The calculations using the generalized means are direct without needing to know bulk or shear moduli separately. However, the calculations of Hashin and Shtrikman bounds require full information on the bulk and shear moduli of each phase of the two-phase composites. A full set of elastic data is usually lacking because only one elastic constant (i.e. Young's, shear or bulk modulus) is often measured for the components (see Berryman (1995) for a review). In the latter cases, the Hashin and Shtrikman's upper and lower bounds cannot be calculated. Moreover, the Hashin–Shtrikman bounds generally lie too far apart to be useful for practical purposes because no effect of the composite microstructure has been taken into consideration. Nevertheless, the generalized means have the advantage that they make use of the microstructure (by choosing properly the J value) to obtain more accurate estimates than the Hashin–Shtrikman bounds. In addition, the validity of the Hashin–Shtrikman bounds actually depends on the relative magnitudes of K_s, K_w, G_s, G_w, ν_s and ν_w, where ν is Poisson's ratio. An inversion of the upper and lower bounds often occurs at high values of K_w/K_s (>0.2) and/or at low values of ν_w/ν_s (<1.0) (Ji and Wang, 1999).

The Hill average has been widely used in the modelling of the overall elastic properties of polycrystalline aggregates

Table 1
J-value as functions of the phase shape and distribution

Shape of inclusion	$\|J\|$	Inclusion as:	Microstructure	J	Examples
Sphere	0.50	Weak phase	SPSS	0.50	Porous glass
		Strong phase	WPSS	−0.50	Dilute suspension in a Newtonian liquid
Random geometry	0.25	Weak phase	SPSS	0.25	Porous Al_2O_3, porous MgO, WC–Co
		Strong phase	WPSS	−0.25	Al–SiC, Al–boron, Al–spinel, epoxy–silica, epoxy–glass, epoxy–Al, glass–Al_2O_3, glass–tungsten

(e.g. Montagner and Anderson, 1989; Zhao and Anderson, 1994; and many others). However, the present study proved that the elastic constants of the composites could not be precisely estimated using the Hill scheme for most two-phase composites investigated.

Although the comparison between theory and experiment was done for the elastic properties, the present approach can be easily extended to the prediction of other mechanical and physical properties of multiphase composites (e.g. flow strength, electrical conductivity and thermal conductivity). Furthermore, unlike many other models that apply to only two-phase composites (e.g. Ji and Zhao, 1994; Ravichandran, 1994; Zhao and Ji, 1997), the present model is also adequate for all composites consisting of more than two phases. We hope that the present study will encourage systematic measurements of the J value for composite materials and rocks with various microstructural characteristics.

Importantly, the generalized means proposed here are obviously advantageous to have an analytical formula rather than a computational one. This advantage is extremely useful if it is desired to invert the elastic data or seismic velocities to the volume fractions of the composite constituent phases and the microstructure. The theory presented in this paper can be used to develop some new techniques to determine how much volume fraction of diamond has formed during the phase transition from graphite in high temperature and high pressure anvils through in-situ, non-destructive acoustic measurements.

As an application, the effect of the structural transition on effective elastic properties of binary olivine–wadsleyite mixtures has been analysed. The analysis suggests that the width of the seismic discontinuity at 410 km should be directly governed by the width of the transition from an olivine-supported structure to a wadsleyite-supported structure rather than that of an experimentally determined binary phase loop. The width of the discontinuity is likely reduced by a factor of three or four with respect to that of the binary coexistence region. The change in effective elastic properties due to the structural transition is effectively much sharper than the width of the binary coexistence region.

Acknowledgements

We thank the NSERC and LITHOPROBE of Canada and Guangzhou Institute of Geochemistry (Chinese Academy of Sciences, KZCXZ-SW-117) for research grants. We appreciate the constructive reviewing comments of J.G. Berryman, T.M. Tharp and C.W. Passchier. This is LITHOPROBE contribution No. 1350.

References

Akaogi, M., Ito, E., Navrotsky, A., 1989. Olivine-modified spinel–spinel transitions in the system Mg_2SiO_4–Fe_2SiO_4: calorimetric measurements, thermochemical calculation, and geophysical application. Journal of Geophysical Research 94, 15671–15685.

Arzi, A.A., 1978. Critical phenomena in the rheology of partially melted rocks. Tectonophysics 44, 173–184.

Benz, H.M., Vidale, J.E., 1993. Sharpness of upper mantle discontinuities determined from high-frequency reflections. Nature 365, 147–150.

Berge, P.A., Bonner, B.P., Berryman, J.G., 1995. Ultrasonic velocity–porosity relationship for sandstone analogs made from fused glass beads. Geophysics 60, 108–119.

Berryman, J.G., 1994. Role of porosity in estimates of composite elastic constants. Journal of Energy Resources Technology 116, 87–96.

Berryman, J.G., 1995. Mixture theories of rock properties. In: Ahrens, T.J., (Ed.), Rock Physics and Phase Relations: A Handbook on Physical Constants, AGU, Washington, DC, pp. 205–228, AGU Ref. Shelf, vol. 3.

Bina, C.R., Kumazawa, M., 1993. Thermodynamic coupling of phase and chemical boundaries. Physics of the Earth and Planetary Interiors 76, 329–341.

Braem, M., Van Doren, V.E., Lambrechts, P., Vanherle, G., 1987. Determination of Young's modulus of dental composites: a phenomenological model. Journal of Material Science 22, 2037–2042.

Chen, P.E., Lin, J.M., 1969. Transverse properties of fibrous composites. Material Research Standards 9, 29–33.

Doi, H., Fujiwara, Y., Miyake, K., Oosawa, Y., 1970. A systematic investigation of elastic moduli of WC–Co alloys. Metallurgical Transactions 1, 1417–1425.

Dziewonski, A.M., Anderson, D.L., 1981. Preliminary reference Earth model. Physics of the Earth and Planetary Interiors 25, 297–356.

Einstein, A., 1906. Eine neue Bestimmung der Molekuldimensionen. Annals of Physics (Leipzig) 19, 289–306.

Einstein, A., 1911. Berichtigung zu meiner arbeit—eine neue Bestimmung der Molekuledimensionen. Annals of Physics (Leipzig) 34, 591–592.

Fei, Y.W., Mao, H.K., Mysen, B.O., 1991. Experimental determination of element partitioning and calculation of phase relations in the MgO–FeO–SiO_2 system at high pressure and high temperature. Journal of Geophysical Research 96, 2157–2170.

Gurland, J., 1979. A structural approach to the yield strength of two-phase alloys with coarse microstructures. Materials Science and Engineering 40, 59–71.

Gustafson, T.W., Panda, P.C., Song, G., Raj, R., 1997. Influence of microstructural scale on plastic flow behavior of metal matrix composites. Acta Materialia 45, 1633–1643.

Hashin, Z., Shtrikman, S., 1963. A variation approach to the theory of the

elastic behavior of multiphase materials. Journal of the Mechanics and Physics of Solids 11, 127–140.

Hasselman, D.P., Fulrath, R.M., 1965a. Effect of alumina dispersion on Young's modulus of a glass. Journal of the American Ceramic Society 48, 218–219.

Hasselman, D.P., Fulrath, R.M., 1965b. Effect of spherical tungsten dispersion on Young's modulus of a glass. Journal of the American Ceramic Society 48, 548–549.

Hill, R., 1963. Elastic properties of reinforced solids: some theoretical principles. Journal of the Mechanics and Physics of Solids 11, 357–372.

Ishai, O., Cohen, L.J., 1967. Elastic properties of filled and porous epoxy composites. International Journal of Mechanical Sciences 9, 539–546.

Jeanloz, R., Thompson, A.B., 1983. Phase transitions and mantle discontinuities. Reviews of Geophysics 21, 51–74.

Ji, S.C., Wang, Z., 1999. Elastic properties of forsterite–enstatite composites up to 3.0 GPa. Journal of Geodynamics 28, 147–174.

Ji, S.C., Xia, B., 2002. Rheology of Polyphase Earth Materials. Polytechnic International Press, Montreal, 260pp.

Ji, S.C., Zhao, P., 1994. Strength of two-phase rocks: a model based on fiber-loading theory. Journal of Structural Geology 16, 253–262.

Ji, S.C., Wirth, R., Rybacki, E., Jiang, Z., 2000. High-temperature plastic deformation of quartz-plagioclase multilayers by layer-normal compression. Journal of Geophysical Research 105, 16,651–16,664.

Ji, S.C., Wang, Z.C., Wirth, R., 2001. Bulk flow strength of forsterite–enstatite composites as a function of forsterite content. Tectonophysics 341, 69–93.

Ji, S.C., Wang, Q., Xia, B., 2002. Handbook of Seismic Properties of Minerals, Rocks and Ores. Polytechnic International Press, Montreal, 630pp.

Ji, S.C., Wang, Q., Xia, B., 2003. P-wave velocities of polymineralic rocks: comparison of theory and experiment and test of elastic mixture rules. Tectonophysics 366, 165–185.

Katsura, T., Ito, E., 1989. The system Mg_2SiO_4–Fe_2SiO_4 at high-pressures and temperatures: precise determination of stabilities of olivine, modified spinel, and spinel. Journal of Geophysical Research 94, 15663–15670.

Kenyon, A.S., Duffey, H.J., 1967. Properties of a particulate-filled polymer. Polymer Engineering and Science 7, 189–193.

Knudson, F.P., 1962. Effect of porosity on Young's modulus of alumina. Journal of the American Ceramic Society 45, 94–95.

Korvin, G., 1982. Axiomatic characterization of the general mixture rule. Geoexploration 19, 267–276.

Lebedev, S., Chevrot, S., van der Hilst, R.D., 2002. Seismic evidence for olivine phase changes at the 410- and 660-kilometer discontinuities. Science 296, 1300–1302.

Lees, A.C., Bukowinski, M.S.T., Jeanloz, R., 1983. Reflection properties of phase transition and compositional change models of the 670-km discontinuity. Journal of Geophysical Research 88, 8145–8159.

Lejeune, A.M., Richet, P., 1995. Rheology of crystal-bearing silicate melts: an experimental study at high viscosities. Journal of Geophysical Research 100, 4215–4229.

Leven, J.H., 1985. The application of synthetic seismograms to the interpretation of the upper mantle P-wave velocity structure in northern Australia. Physics of the Earth and Planetary Interiors 38, 9–27.

Lloyd, D.J., 1991. Aspects of fracture in particulate reinforced metal matrix composites. Acta Metallurgica et Materialia 39, 59–71.

Mainprice, D., Humbert, M., 1994. Methods of calculating petrophysical properties from lattice preferred orientation data. Surveys in Geophysics 15, 575–592.

Matthies, S., Humbert, M., 1993. The realization of the concept of a geometric mean for calculating physical constants of polycrystalline materials. Physica Status Solidi B177, K47–K50.

McDanels, D.L., 1985. Analysis of stress-strain, fracture and ductility of aluminium matrix composites containing discontinuous silicon carbide reinforcement. Metallurgical Transactions 16A, 1105–1115.

Mewis, J., Macosko, C.W., 1994. Suspension rheology. In: Macosko, C.W., (Ed.), Rheology: Principles, Measurements and Applications, VCH, New York, pp. 425–474.

Montagner, J.P., Anderson, D.L., 1989. Constrained reference mantle model. Physics of the Earth and Planetary Interiors 58, 205–227.

Paul, B., 1960. Prediction of elastic constants of multiphase materials. Transactions of the Metallurgical Society of AIME 218, 36–41.

Paulssen, H., 1988. Evidence for a sharp 670-km discontinuity as inferred from P-to-S converted waves. Journal of Geophysical Research 93, 10, 489–10,500.

Perrott, C.M., 1978. On the indentation fracture of cemented carbide II—the nature of surface fracture toughness. Wear 47, 81–91.

Ravichandran, K.S., 1994. Elastic properties of two-phase composites. Journal of the American Ceramic Society 77, 1178–1184.

Richard, T.G., 1975. The mechanical behavior of a solid microsphere filled composite. Journal of Composite Materials 9, 108–113.

Rutter, E.H., Neumann, D.H.K., 1995. Experimental deformation of partially molten Westerly granite under fluid-absent conditions, with implications for the extraction of granitic magma. Journal of Geophysical Research 100, 15697–15715.

Smith, J.C., 1976. Experimental values for the elastic constants of a particulate-filled glassy polymer. Journal of Research of the National Bureau of Standards—A. Physics and Chemistry 80A, 45–49.

Solomatov, V.S., Stevenson, D.J., 1994. Can sharp seismic discontinuities be caused by nonequilibrium phase transitions? Earth and Planetary Science Letters 125, 267–279.

Spriggs, R.M., 1961. Expression for effect of porosity on elastic modulus of polycrystalline refractory materials, particularly aluminium oxide. Journal of the American Ceramic Society 44, 628–629.

Spriggs, R.M., Brissette, L.A., Vasilos, T., 1962. Effect of porosity on elastic and shear moduli of polycrystalline magnesium oxide. Journal of the American Ceramic Society 45, 400–405.

Stixrude, L., 1997. Structure and sharpness of phase transitions and mantle discontinuities. Journal of Geophysical Research 102, 14835–14852.

Tharp, T.M., 1983. Analogies between the high-temperature deformation of polyphase rocks and the mechanical behavior of porous powder metal. Tectonophysics 96, T1–11.

Treagus, S.H., 2002. Modeling the bulk viscosity of two-phase mixtures in terms of clast shape. Journal of Structural Geology 24, 57–76.

Tullis, T., Horowitz, F.G., Tullis, J., 1991. Flow laws of polyphase aggregates from end-member flow. Journal of Geophysical Research 96, 8081–8096.

Walsh, J.B., Brace, W.F., England, A.W., 1965. Effect of porosity on compressibility of glass. Journal of the American Ceramic Society 48, 605–608.

Watt, J.P., O'Connell, R.J., 1980. An experimental investigation of the Hashin–Shtrikman bounds on two-phase aggregate elastic properties. Physics of the Earth and Planetary Interiors 21, 359–370.

Wood, B.J., 1995. The effect of H_2O on the 410-kilometer seismic discontinuity. Nature 268, 74–76.

Wyllie, M.R.J., Gregory, A.R., Gardner, L.W., 1956. Elastic wave velocities in heterogeneous and porous media. Geophysics 21, 41–70.

Yang, J., Pickard, S.M., Cady, C., Evans, A.G., Mehrabian, R., 1991. The stress/strain behavior of aluminum matrix composites with discontinuous reinforcements. Acta Metallurgica et Materialia 39, 1863–1869.

Zhang, M., Ebrom, D.A., McDonald, J.A., Tatham, R.H., 1996. Comparison of experimental velocity measurements with theoretical results in a solid-solid composite material. Geophysics 61, 1429–1435.

Zhao, P., Ji, S.C., 1997. Refinements of shear-lag model and its applications. Tectonophysics 279, 37–53.

Zhao, Y., Anderson, D.L., 1994. Mineral–physical constraints on the chemical composition of the Earth's lower mantle. Physics of the Earth and Planetary Interiors 85, 273–292.